# Electronic structure of the $Ti_4O_7$ Magnéli phase

Leandro Liborio* and Giuseppe Mallia
*TYC, The London Centre for Nanotechnology, Imperial College London, London SW7 2AZ, United Kingdom*

Nicholas Harrison
*TYC, The London Centre for Nanotechnology, Imperial College London, London SW7 2AZ, United Kingdom and STFC, Daresbury Laboratory, Daresbury, Warrington WA4 4AD, United Kingdom*

(Received 21 November 2008; revised manuscript received 1 June 2009; published 29 June 2009)

We have performed density-functional calculations on the $Ti_4O_7$ Magnéli phase. Our results provided a consistent description of the high-temperature ($T \geq 298$ K) phase, the intermediate-temperature (120 K $\leq T \leq 140$ K) phase, and the low-temperature ($T \leq 120$ K) phase. The established model for the electronic structure of the low- and intermediate-temperature phases of $Ti_4O_7$ states that $Ti^{3+}$-$Ti^{3+}$ pairs, bonded through nonmagnetic metal-metal bonds, form ordered bipolarons in the low-temperature phase, and that these bipolarons exist but are disordered in the intermediate-temperature phase. In this work we propose a different picture for the $Ti_4O_7$ low- and intermediate-temperature electronic structure. We argue that, in the low-temperature phase, a combination of a strong on-site Coulomb repulsion and electron-phonon coupling results in the localization of unpaired electrons in the $Ti^{3+}$ ions forming the pairs. The electrons are accommodated in specific $t_{2g}$-like orbitals for two reasons: to minimize the direct Coulomb repulsion, and to minimize the indirect interaction that results from lattice distortion. The localized electrons are antiferromagnetically coupled, producing bipolarons with zero spin. This orbital ordering results in the widening of the gap between the fully occupied and unoccupied levels. This is a bipolaronic state, but there is no bond in between the $Ti^{3+}$ forming the pairs. In the intermediate phase, a subset of the bipolarons dissociate but the electrons remain strongly localized: this state consists of a mixture of polarons and bipolarons placed in a superstructure with long-range order. This model provides a consistent explanation of the observed electric and magnetic properties of $Ti_4O_7$.

DOI: 10.1103/PhysRevB.79.245133 PACS number(s): 71.15.−m, 71.38.Mx, 71.55.−i, 74.62.Dh

## I. INTRODUCTION

Magnéli phases are a substoichiometric composition of titanium oxides. They form a homologous series $Ti_nO_{2n-1}$ whose end members—$TiO_2$ and $Ti_2O_3$—show marked differences in their crystalline structures as well as in their magnetic and electrical properties. Moreover, there is a strong correlation between changes in the crystalline structure and changes in the physical properties.

The crystalline structure of the Magnéli phases can be viewed as rutile-type slabs of infinite extension and different thickness, separated by shear planes with a corundum-like atomic arrangement.[1] When moving from $TiO_2$ to $Ti_2O_3$ in the Ti-O phase diagram,[2] the *d* band occupation across the series increases and the material electronic structure changes. The changing electronic structure has profound consequences in the temperature dependence of physical properties such as the magnetic susceptibility and the electrical conductivity.

Bartholomew and Frankl[3] measured the electrical conductivity of $Ti_nO_{2n-1}$ with $3 \leq n \leq 6$ within the temperature range 78–298 K. Inglis *et al.*[4] studied the temperature dependence of the electrical conductance of $Ti_nO_{2n-1}$ with $4 \leq n \leq 9$ in the 4–320 K temperature range. In these studies no single conduction mechanism was found to dominate across the series. In particular, for $Ti_4O_7$, both works reported discontinuities in the conductivity as the temperature was changed: a semiconductor-semiconductor transition in the 125–140 K temperature range and a semiconductor-metal transition at about 150 K. It is in this Magnéli phase, $Ti_4O_7$, where the bulk of the analysis, regarding the study of the metal-semiconductor and semiconductor-semiconductor transition, has been focused.

Marezio *et al.*[5] performed single-crystal x-ray investigations on $Ti_4O_7$ as it went through the semiconductor-metal and semiconductor-semiconductor transitions. Through this accurate determination of the crystalline structures, they estimated the charge of the titanium ions by comparing the average titanium-oxygen interatomic distance, in each titanium-oxygen octahedron, with the $Ti^{3+}$, $Ti^{4+}$, and $O^{2-}$ Shannon and Prewitt[6] ionic radii. The resulting charge distribution suggested that, at $T \leq 140$ K, there is a clear separation into chains of alternating $Ti^{3+}$ and $Ti^{4+}$ ions, with $Ti^{3+}$ ions accommodated in a long-range-ordered arrangement of $Ti^{3+}$-$Ti^{3+}$ pairs. The interatomic distance between these titanium atoms is shorter than in bulk rutile. On the other hand, in the so-called high-temperature phase, when $T \geq 150$ K, pairing is absent and all the titanium sites are similar and were interpreted as containing $Ti^{3.5+}$ ions.

In between the low and high-temperature phases, Marezio *et al.*[5] first suggested that, at 140 K $\leq T \leq 150$ K, the $Ti^{3+}$-$Ti^{3+}$ pairs still exist, but their long-range order has vanished. In a subsequent work Marezio and Page[7] revisited the $Ti_4O_7$ structure at its three different phases. The low and high-temperature structures were equivalent to the ones previously reported, but they reported a new structure for the 140 K phase. Contrary to the previous ones, this structure showed long-range order of the Ti valences and pairing of the $Ti^{3+}$ atoms. Their conclusion was that, at 140 K, bipolarons were still present, but they were not disordered.

 

Lakkis *et al.*[8] combined x-ray diffraction with electron-paramagnetic-resonance studies. They discussed the nature of the $Ti_4O_7$ electronic structure in its different phases and proposed a mechanism for the semiconductor-metal and semiconductor-semiconductor transitions. They represented the low temperature $Ti^{3+}$-$Ti^{3+}$ pairs as small on-site localized *bipolarons*.[9,10] These are bound states of two $Ti^{3+}$ ions stabilized by a lattice distortion.

Lakkis *et al.*[8] assumed that, in the low and intermediate temperature phases, the titanium 3*d* electrons forming the bipolarons were paired in nonmagnetic metal-metal bonds. Using the bipolaron concept, they interpreted the 140 K semiconductor-semiconductor transition in terms of a disordering of the $Ti^{3+}$-$Ti^{3+}$ bonds: the bipolarons were considered to be mobile within the crystalline network without breaking.

The result of the studies is that there are two competing models. One model, proposed by Lakkis *et al.*,[8] considered that all the bipolarons, which were well ordered in the low-temperature phase, remained in the intermediate phase, but they were disordered. The other model proposed the opposite: on the basis of x-ray measurements, Marezio and Page[7] suggested there had to be a long-range order for the $Ti^{3+}$ ions and, consequently, the bipolarons.

Within both these models, the observed electron-paramagnetic signals were difficult to explain. Therefore, Lakkis *et al.*[8] postulated that the EPR signals were originated in additional dilute $Ti^{3+}$ magnetic centers, which were located on normal $Ti^{3+}$ sites.

Finally, at $T \geq 150$ K, all proposed models attributed the metallic behavior to a delocalization of the 3*d* electrons.

The optical properties of $Ti_4O_7$ have also been investigated. Kaplan *et al.*[11] performed experimental optical measurements on $Ti_4O_7$ in the temperature range of the semiconductor-metal transition. They obtained a value of 0.25 eV for the optical band gap and related it to the so-called interchain optical transitions: these are the optical excitations corresponding to taking an electron out of a $Ti^{3+}$ pair to an empty neighboring $Ti^{4+}$ site.

More recently, Watanabe *et al.*[12] measured $Ti_4O_7$ reflection spectra as a function of temperature. They found it changed discontinuously at the electronic phase-transitions temperatures of 130 and 150 K, and attributed these changes to the formation of bipolarons.

Surprisingly, in spite of the significant body of experimental work, there are very few *ab initio* calculations on the Magnéli phases. Recently, two of us[13] studied the equilibria between the $Ti_nO_{2n-1}$ $(4 \leq n \leq 9)$ Magnéli phases using *ab initio* thermodynamics. The predicted phase stability was in very good agreement with that observed, and it was used to assess one of the mechanisms proposed to explain the formation of the Magnéli phases in rutile.

Previous to this paper there were, to the best of the authors' knowledge, only two *ab initio* studies. Leonov *et al.*[14] performed LDA+*U* calculations on $Ti_4O_7$ low-temperature structure. They investigated $Ti_4O_7$ charge ordering and, with $U=3.0$ eV, found a charge-ordered insulating solution with an energy gap of 0.29 eV, in agreement with the optical spectra. Eyert *et al.*[15] performed local spin density approximation (LSDA) band-structure calculations on the same low-temperature structure. Although these calculations provided information about the composition of the bands in terms of the atomic orbitals, they failed to reproduce an insulating spin-singlet ground state.

Hence, we believe that only a theoretical treatment, in which structural aspects as well as correlations within the Ti-Ti pairs are considered on the same basis, can decide on the underlying mechanism for the metal-semiconductor and semiconductor-semiconductor transitions in the $Ti_4O_7$ Magnéli phase. To address this issue, we have performed hybrid exchange density functional calculations using the CRYSTAL code.[16]

## II. COMPUTATIONAL DETAILS

All calculations have been performed using the CRYSTAL06 software package,[16] based on the expansion of the crystalline orbitals as a linear combination of a local basis set (BS) consisting of atom centered Gaussian orbitals. The titanium and oxygen atoms are described by a triple valence all-electron BS: an 86-411G** contraction (one *s*, four *sp*, and two *d* shells) and an 8-411G* contraction (one *s*, three *sp*, and one *d* shells), respectively;[17] the most diffuse *sp*(*d*) exponents are $\alpha^{Ti}=0.3297(0.26)$ and $\alpha^{O}=0.1843(0.6)$ bohr$^{-2}$. These basis sets were developed in previous studies of the bulk and surfaces phases of titania in which a systematic hierarchy of all-electron basis sets was used to quantify the effects of using a finite BS;[18,19] in addition they were adopted in a previous work.[20]

Electron exchange and correlation are approximated using the B3LYP hybrid exchange functional[21] which, as noted above, is expected to be more reliable than local-density approximation (LDA) or generalized gradient approximation (GGA) approaches. The exchange-correlation potential and energy are integrated numerically on an atom centered grid of points. The integration over radial and angular coordinates is performed using Gauss-Legendre and Lebedev schemes, respectively. A pruned grid consisting of 75 radial points and 5 subintervals with (50,146,194,434,194) angular points has been used for all calculations [the LGRID option implemented in CRYSTAL06 (Ref. 16)]. The Coulomb and exchange series are summed directly and truncated using overlap criteria with thresholds of $10^{-7}$, $10^{-7}$, $10^{-7}$, $10^{-7}$, and $10^{-14}$ as described previously.[16,22] Reciprocal space sampling was performed on a Pack-Monkhorst net with a shrinking factor, IS=4, which defines a set of *k* points in the Brillouin zone (BZ). The self-consistent field procedure was converged to a tolerance in the total energy of $\Delta E=1\cdot10^{-7}E_h$ per unit cell.

As was mentioned in the introduction, $Ti_4O_7$ suffers a semiconductor-metal transition at around 150 K and a semiconductor-semiconductor transition at around 120 K. Each one of this phases has an associated triclinic crystalline structure. In this work we have calculated the band-structure and spatial electronic density for each one of them, taking the atomic coordinates from.[5] The $Ti_4O_7$ unit cell has eight titanium and 14 oxygen atoms.

## III. RESULTS AND DISCUSSION

The electronic structure of $Ti_4O_7$ is strongly coupled to the lattice distortions. For instance: the distortion of the oxy-

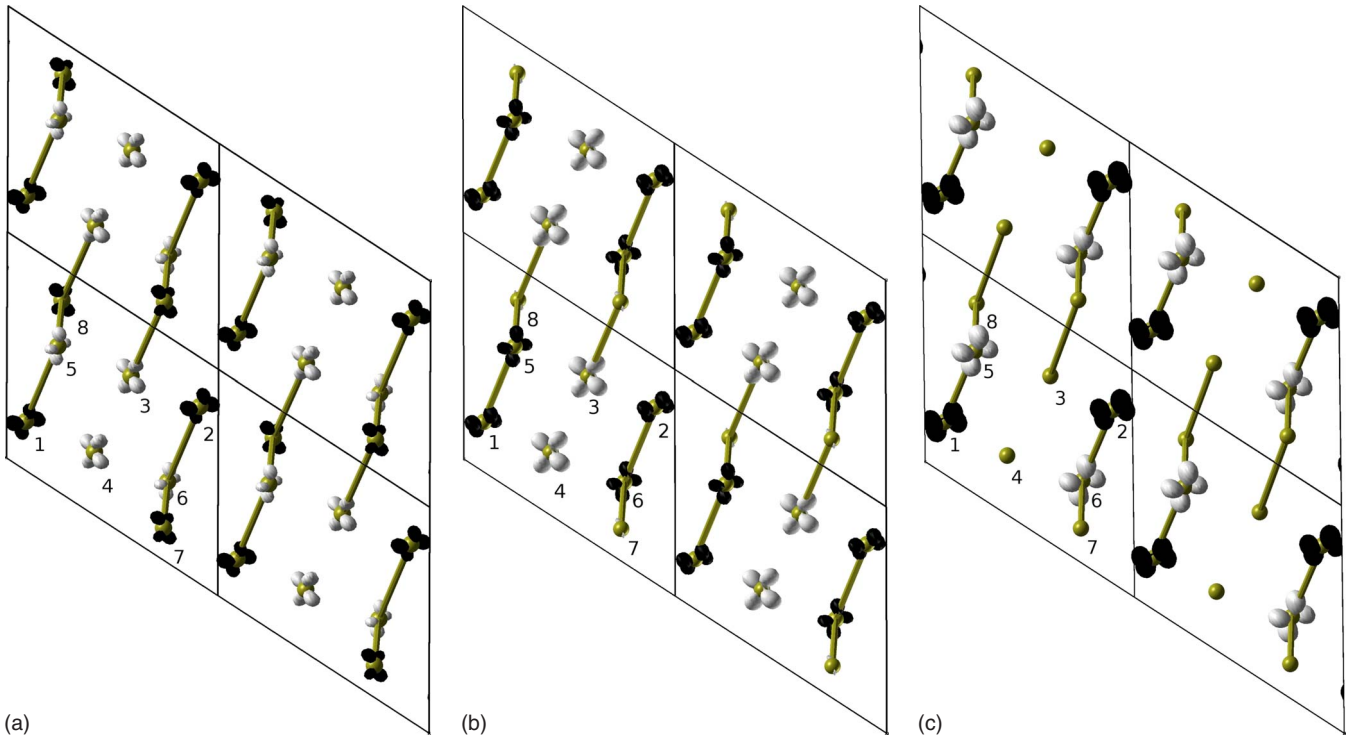


FIG. 1. (Color online) (a)–(c) are $Ti_4O_7$ crystal structures showing only Ti atoms. These figures show a view of a $(1\times2\times2)$ $Ti_4O_7$ supercell along the tetragonal $Ti_4O_7$ unit cell *a* axis. The figure is divided into its unit-cell components and all the titanium atoms are labeled. (a) shows the high-temperature phase ($T>298$ K), (b) indicates the intermediate phase ($T<140$ K), and (c) represents the low-temperature phase ($T<120$ K). The black and white shapes represent $\pm0.05(\frac{e}{\text{bohr}^3})$ spin isodensity surfaces.

gen octahedra around each one of the inequivalent titanium atoms influences their electronic density. It is therefore important to discuss the electronic structures, and resulting properties, of each of the experimental structures presented by Marezio *et al.*[5] and Marezio and Page[7] in some detail. To achieve this, we performed consistent total-energy calculations for the crystalline structures of $Ti_4O_7$ in its three phases—as reported by Marezio *et al.*[5]—and in its intermediate phase structure, as reported by Marezio and Page.[7]

### A. Structures of the low-, intermediate-, and high-temperature phases of $Ti_4O_7$

Figure 1 shows a view of a $(1\times2\times2)$ $Ti_4O_7$ supercell along the tetragonal $Ti_4O_7$ unit cell *a* axis.[5] In the interests of clarity, we have removed all the oxygen atoms from this figure: only titaniums are shown. One of the $Ti_4O_7$ unit cells in each of the $(1\times2\times2)$ supercells has all the titanium atoms labeled. There are 8 titanium atoms depicted, and they can be divided in four inequivalent pairs of symmetry related titanium atoms: $\text{Ti}(1)\equiv\text{Ti}(2)$; $\text{Ti}(3)\equiv\text{Ti}(4)$; $\text{Ti}(5)\equiv\text{Ti}(6)$; $\text{Ti}(7)\equiv\text{Ti}(8)$. The yellow bonds indicate the titanium connectivity among the closest pairs of titanium atoms. The behavior of two of these distances, plus the Ti(8)-Ti(3) distance, are documented in Table I. Table II shows the average Ti-O distances at the different temperatures.

At the 150 K transition only small displacements occur. Comparing equivalent octahedra at 298 and 140 K, it can be seen that the Ti(1) and Ti(5) octahedra expand, whereas the Ti(3) and Ti(8) octahedra contract. This tendency is maintained as the temperature is decreased below 125 K (Table II).

Table III shows the computed distribution of spin moments on each of the inequivalent titanium atoms for the Marezio *et al.*[5] $Ti_4O_7$ structures.[23] The system is antiferromagnetic at all the observed temperatures, and the spin moment on each of the titaniums forming the $Ti^{3+}$-$Ti^{3+}$ pairs at 120 K—Ti(1) and Ti(5)—increases in absolute value when moving from 298 to 120 K.

Moreover, the Mulliken bond population $(q=n_\alpha+n_\beta)$ between the Ti-Ti pairs, indicated in Table I, is below $0.01\frac{e}{\text{bohr}^3}$ in all the $Ti_4O_7$ phases considered.

The spin localizes in the titanium $t_{2g}$-like orbitals in the local reference frame of the $TiO_6$ octahedra. These orbitals result from the crystal field splitting of the titanium states

TABLE I. Comparison between Ti-Ti distances at the different temperatures. The Ti atoms considered here are the ones where the spin tends to be localized. The labels on the first column refer to titanium pairs in Fig. 1.

| | Ti-Ti distances (Å) | | |
|---|---|---|---|
| Ti pairs | 298 K | 140 K | 120 K |
| 8–3 | 3.067 | 3.101 | 3.104 |
| 8–5 | 2.812 | 2.806 | 2.837 |
| 5–1 | 3.019 | 2.990 | 2.802 |

TABLE II. Average Ti-O distances, for the four inequivalent titanium atoms, at the different temperatures as reported by Marezio *et al.* (Ref. 5).

| | Ti-O average distance (Å) | | |
|---|---|---|---|
| Ti atom | 298 K | 140 K | 120 K |
| 1 | 2.006 | 2.011 | 2.043 |
| 3 | 2.006 | 2.000 | 1.973 |
| 5 | 2.004 | 2.015 | 2.044 |
| 8 | 2.018 | 2.012 | 1.996 |
| Overall average | 2.008 | 2.009 | 2.014 |

and point away from the oxygens in the surrounding octahedron.

Figure 2 shows the spin distribution documented in Table III as isovalue surfaces. These figures show a view of the $Ti_4O_7$ unit cell along its *a* axis: the same point of view depicted in Fig. 1, but with some representative oxygen atoms included. The spin isodensity surfaces are indicated in black ($-0.05e/\text{bohr}^3$) and white ($0.05e/\text{bohr}^3$). Figures 2(a) and 2(b) represent the spin distribution at 298 and 140 K, respectively. Similarly, Figs. 2(c) and 2(d) portray the spin distribution at 140 and 120 K. In each one of these pair of figures the most representative oxygen octahedra have been plotted, namely: the ones neighboring the titanium atoms where the spin localizes after the phase transition.

At room temperature the average Ti-O distance in $Ti_4O_7$ is 2.008 Å (see Table II), whereas in bulk rutile it is 1.9641 Å.[24] Marezio *et al.*[5] linked this increase in the associated octahedra volume with the new titanium charged state, $Ti^{3.5+}$, and its larger effective radius. The rather homogeneous spin distribution computed at the 298 K geometry (Table III) is consistent with this picture.

At the 150 K transition the electronic density increases at Ti(3) by ≈50%, and the net effect is to decrease, albeit slightly (see Table II), the volume of its associated oxygen octahedra.

Decreasing the temperature further, at the 125 K phase transition, the electronic density is concentrated mostly on Ti(1) and Ti(5). The associated oxygen octahedra share an edge and the spin on each titanium $t_{2g}$-like orbital has opposite sign. From Table I it can be seen that these titanium atoms are nearest neighbors, with an interatomic distance slightly smaller than the distance in rutile $TiO_2$ bulk (2.9 Å at 298 K).

TABLE III. Titanium *d* orbitals spin population. The spin, $\mu = n_\alpha - n_\beta$, is measured in bohr magnetons.

| | $\mu = n_\alpha - n_\beta$ | | |
|---|---|---|---|
| Ti atom | 298 K | 140 K | 120 K |
| 1 | −0.449 | −0.442 | −0.872 |
| 3 | 0.420 | 0.672 | −0.026 |
| 5 | 0.331 | −0.380 | 0.875 |
| 8 | −0.303 | 0.126 | 0.039 |

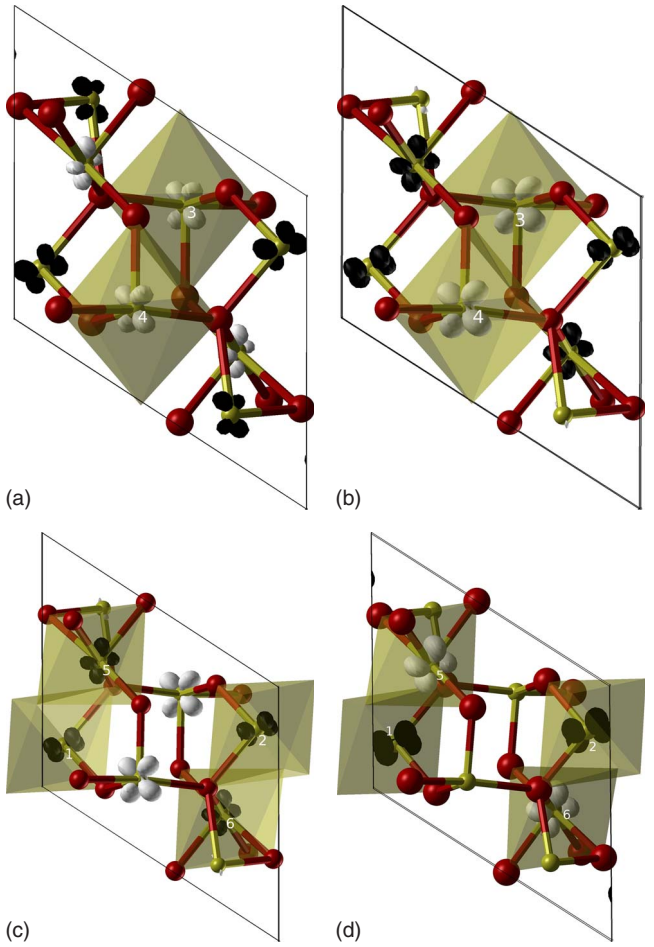


FIG. 2. (Color online) (a)–(d) show a view of the $Ti_4O_7$ unit cell along its *a* axis. These figures are essentially similar to Fig. 1, but in this case some representative oxygens are included as well. (a) and (b) indicate the spin distribution at 298 and 140 K, (c) and (d) do it at 140 and 120 K. For clarity, only oxygen octahedra corresponding to titanium atoms where the spin is placed are plotted.

The data in Table I and Figs. 1(c) and 2(d) indicate the "dimerization pattern" of the low-temperature phase, that is, the ordering of the titanium $t_{2g}$-like orbitals in space. Table I also indicates a correlation between the change in the interatomic Ti-Ti distance and its associated ionic charge: titanium atoms in the $Ti^{3+}$-$Ti^{3+}$ pairs [for instance, Ti(1) and Ti(5)] are closer than titanium atoms in the $Ti^{3+}$-$Ti^{4+}$ pairs [for instance, Ti(3) and Ti(5)].

The qualitative picture that emerges of the $Ti_4O_7$ low-temperature state is that of a bipolaronic state, but the bipolarons are not *covalently* bonded: the spin localizes in $t_{2g}$-like orbitals belonging to $Ti^{3+}$ ions and these ions are antiferromagnetically coupled.

### B. Marezio and Page 140 K intermediate structure

Figure 3 shows a $(1\times2\times2)$ supercell of the 140 K $Ti_4O_7$ structure measured by Marezio and Page.[7] In Fig. 3(a) only the titanium atoms are displayed, and the yellow bonds indicate the titanium connectivity among the closest pairs of titanium atoms. Among all these pairs, we are particularly

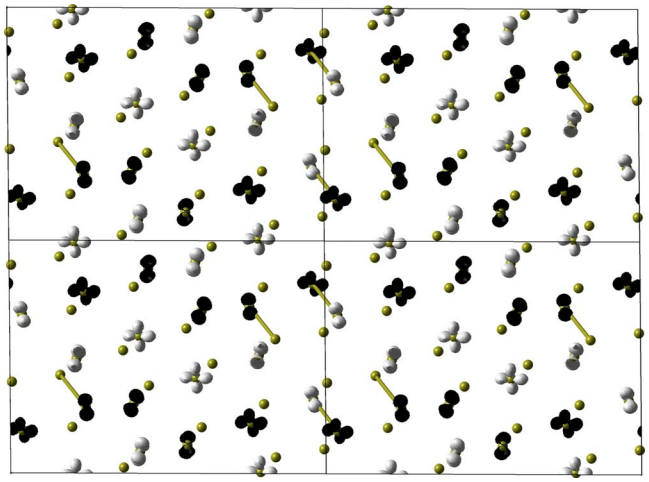
(a)

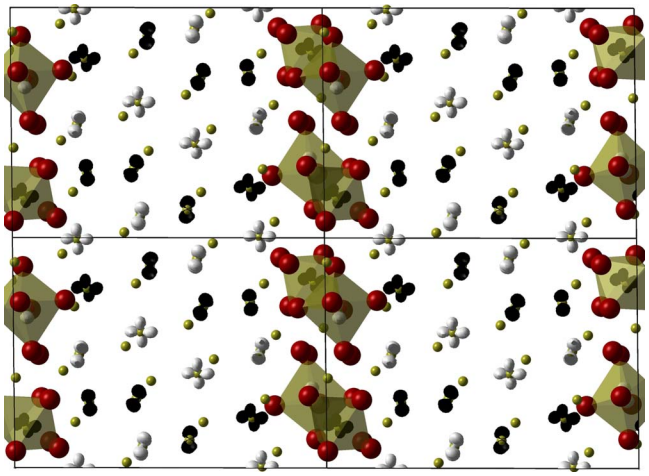
(b)

FIG. 3. (Color online) (a) and (b) show a view of a $(1\times2\times2)$ $Ti_4O_7$ supercell along the tetragonal $Ti_4O_7$ unit cell $a$ axis. This supercell corresponds to the 140 K structure obtained by Marezio and Page (Ref. 7). (a) is $Ti_4O_7$ crystalline structure showing only Ti atoms. (b) is essentially the same, except that it includes some representative oxygens. These oxygens define the oxygen octahedra surrounding the titaniums conforming the bipolarons. The black and white shapes represent $\pm0.05(\frac{e}{\text{bohr}^3})$ spin isodensity surfaces.

interested in the ones forming bipolarons. These pairs have their corresponding oxygen octahedra plotted in Fig. 3(b), and it can be seen that these octahedra share a face.

Through the interpretation of their x-ray experiments for $Ti_4O_7$, at 140 K, Marezio and Page[7] proposed a long-range order of titanium valences involving pairing of $Ti^{3+}$ ions. The calculated spin density showed in Fig. 3(a) is localized on $t_{2g}$-like orbitals on $Ti^{3+}$, and is consistent with the ordering observed by Marezio and Page.[7] In Fig. 3(a), the closest pair of atoms—placed at a distance of 2.747 Å—are linked together. Not all of these linked atoms are $Ti^{3+}$: the linked atoms forming the $Ti^{3+}$ pairs have their corresponding oxygen octahedra surrounding them. Figure 3(b) clearly shows that these neighboring octahedra are sharing a face, and that the spin localized on each $Ti^{3+}$ has opposite sign.

Table IV shows the spin moments and the average Ti-O distance only on each of the titanium ions forming the pairs.

TABLE IV. Spin population and Ti-O average distances for the $Ti^{3+}$ forming the bipolarons. The electrons are placed in the titanium $d$ orbitals, and the spin, $\mu=n_\alpha-n_\beta$, is measured in bohr magnetons $\mu_B$.

| Ti atom | Ti-O average distance (Å) | $\mu_B$ |
|---|---|---|
| Ti↑ | 2.034 | 0.788 |
| Ti↓ | 2.033 | −0.751 |

But it is clear from Figs. 3 that there are many more titaniums with spin localization in their $t_{2g}$-like orbitals. In fact, there is spin localization on half of the titaniums in the supercell, with spin moment values ranging from $\pm0.734$ $\mu_B$ up to $\pm0.837$ $\mu_B$.

The spin localization pattern in this 140 K structure[7] is similar to the one observed previously in the 120 K structure:[5] the system is antiferromagnetic and the spin is localized in $t_{2g}$-like orbitals belonging to $Ti^{3+}$ ions. Only a subset of these $Ti^{3+}$ ions form antiferromagnetically bonded pairs and, therefore, the electronic structure at 140 K is not a bipolaronic state: there is a mixture of polarons and bipolarons.

The behavior of $Ti_4O_7$ magnetic properties with temperature will be discussed in more detail in the next section.

### C. Magnetic properties

The magnetic properties of $Ti_4O_7$ have been characterized by magnetic-susceptibility measurements[8,25] and electron-paramagnetic-resonance studies (EPR).[8] All of these experimental results on the susceptibility data show a transition at around 150 K without any measurable hysteresis: the magnetic susceptibility jumps from a constant value of $\approx250\frac{\text{emu}}{\text{mole}}$ to a value of $\approx750\frac{\text{emu}}{\text{mole}}$ and, as the temperature increases further, the system displays paramagnetic behavior.[8]

The EPR spectrum, measured at 80 K by Lakkis *et al.*,[8] shows four principal lines. Of these four lines only one could be followed up to the 140 K transition: after that temperature, its intensity started decreasing. A subsequent EPR measurement at 80 K, performed by the same group but using a different field orientation, detected a hyperfine structure for the aforementioned line. The intensity of this line decreased with temperature and, at $T\geq140$ K, it was no longer detectable.

Lakkis *et al.*[8] assumed the magnetic susceptibility at $T\leq150$ K was of Van Vleck type,[26] and that it was due to the matrix elements between the singlet and triplet states of the $Ti^{3+}$-$Ti^{3+}$ pairs forming the bipolarons.

The experimental results showed that $Ti_4O_7$ magnetic susceptibility did not change at the semiconductor-semiconductor transition that took place in the 120–140 K temperature range.[25] Lakkis *et al.*[8] linked these results with their molecular model for the bipolarons bonding. In their interpretation, the lack of change in the magnetic susceptibility with temperature indicated that (1) the extra electrons at $Ti^{3+}$ remained coupled in the bonding state, and (2) the $Ti^{3+}$-$Ti^{3+}$ distance was the same in the low and intermediate temperature phases.

Our results provide an alternative explanation for the behavior of $Ti_4O_7$ susceptibility with temperature.

As the temperature increases it is clear that, after the 140 K transition, the system remains antiferromagnetic[27] but half of the bipolarons dissociate: the spins are reorganized into bipolarons and polarons. However, the spin remains strongly localized, spatially ordered and its value relatively constant (compare the 120 K values in Table III) and the 140 K values in Table IV).

Moreover, in order to establish the energy scale for spin fluctuations, for the 140 K structure we have calculated the total energy of different magnetically ordered states, i.e.: (a) a ferromagnetic state, (b) a state where we flipped only the spin of half of the electrons forming bipolarons, and (c) a state where we flipped the spin of half of the electrons forming polarons. The lowest energy necessary for changing from the antiferromagnetic ground state to one of these other states was of the order of 0.1 eV per $Ti_4O_7$ unit cell. Such a fluctuation cannot be thermally activated at 140 K, which is consistent with the magnetic susceptibility being constant during the low-temperature transition.

At $T \leq 140$ K the on-site Coulomb energy is strong enough to maintain all the unpaired electrons strongly localized and forming bipolarons. In the $140\ \text{K} \leq T \leq 150$ K temperature range the strong localization remains, but the $Ti^{3+}$-$Ti^{3+}$ pairing is reduced.

The links in between titanium atoms in Fig. 3(a) denote which of these atoms are the closest. It is clear from this figure that not all of these atoms form bipolarons.

The high-temperature phase was considered by Lakkis *et al.*[8] to be metallic. Therefore, they attributed the increase in the magnetic susceptibility to a Pauli term.[28] Again, we propose a different explanation for the room-temperature susceptibility.

Figure 1(a) clearly shows that, at $T \geq 150$ K, the spin is delocalized over all the titanium atoms in the supercell. Moreover, comparing the spin moment values from the 298 K data in Table III with the 140 K spin values from Table IV, it is clear that the value of the spin on each titanium atom has almost halved at room temperature. Clearly, now that the bipolarons have dissociated, the system will behave as a paramagnetic semiconductor; it will be easier to spin polarize and, therefore, the room-temperature magnetic susceptibility is likely to increase at $T \geq 150$ K, in qualitative agreement with the experimental data. The model proposed here also provides an explanation of the EPR data.

The Lakkis *et al.*[8] model of bonded bipolarons for the $T \leq 150$ K phases does not have any unpaired $3d$ electrons. This implies that there was no intrinsic EPR signal to be expected from $Ti_4O_7$ at $T \leq 150$ K. Therefore, Lakkis *et al.*[8] attributed the measured EPR signals, and its subsequent vanishing at a temperature slightly larger than 140 K, to diluted $Ti^{3+}$ magnetic centers whose unpaired electrons have a lifetime smaller than $10^{-10}$ s.

The model proposed here is consistent with the EPR data without invoking additional spin centers. For the $T=120$ K and $T=140$ K structures our model provides strongly localized unpaired electrons, whose spin value kept constant: these electrons are certainly a source of an intrinsic EPR signal.

Finally, in Table III we can see that the value of the spin on each titanium atom has almost halved at room temperature. This is in good agreement with the abrupt decrease in the EPR signal detected experimentally at $T \approx 140$ K.

### D. Density of states

In Fig. 4(c) the low temperature projected density of states (PDOS) for $Ti_4O_7$ is plotted.

The Fermi level is at the zero of energy, and the occupied states just below it are related with the titanium $d$ orbitals of the atoms forming the bipolarons: Ti(1) and Ti(5). These states are strongly localized and form a prominent structure with a band width of 0.5 eV. The computed low-temperature fundamental band-gap is 1.5 eV.

Figures 4(a) and 4(b) show the room and intermediate temperature density of states (DOS) for $Ti_4O_7$ corresponding to the structures proposed by Marezio *et al.*[5] For these structures, the intermediate temperature DOS is very similar to the room-temperature one.

At room and intermediate temperature, the unpaired electrons are distributed over the d levels of all the titanium atoms, and the valence and conduction bands are made up from contributions of titanium atoms. Moreover, the ground state for these structures has an antiferromagnetic configuration with a 0.4 eV band gap and, most importantly, the bipolarons have dissociated. From the PDOS point of view, the low and intermediate phase structures are essentially the same. This appears to contradict the experiments, which suggest that the conductivity of the intermediate phase increases in two orders of magnitude with respect to the low-temperature phase.[8] It was only with the new 140 K structure, proposed by Marezio *et al.*,[5] that experiments could be interpreted.

Figure 5 shows the PDOS for 140 K structure. The system has a 1 eV band-gap, which is 0.6 eV larger than the one computed in the 140 K structure proposed by Marezio and Page.[7] This band-gap opens because the unpaired electrons localize [see Fig. 3(b)].

A band gap that decreases with increasing temperature is in better agreement with the experimental results on the $Ti_4O_7$ electrical conductivity[8] and optical properties.[12] These calculations therefore support the new 140 K structure, proposed by Marezio and Page.[7]

### E. Low-temperature band gap

The reported experimental data for the low-temperature band gap are inconsistent with each other.

Mulay and Danley[25] quote a value of 0.041 eV obtained from conductivity measurements. By means of a combination of photoemission (PES) and O $1s$ x-ray-absorption spectra (XAS), Abbate *et al.*[29] measured the room temperature $Ti_4O_7$ band gap to be 0.6 eV. According to their data, the onset of the O $1s$ XAS did not change at the low-temperature semiconducting phase, which was interpreted as a indication that the Fermi level was pinned at the bottom of the conduction band. From this alternative point of view, they suggested a value of 0.25 eV for the low-temperature band gap, which is in agreement with the value obtained by Kaplan *et al.*,[11]

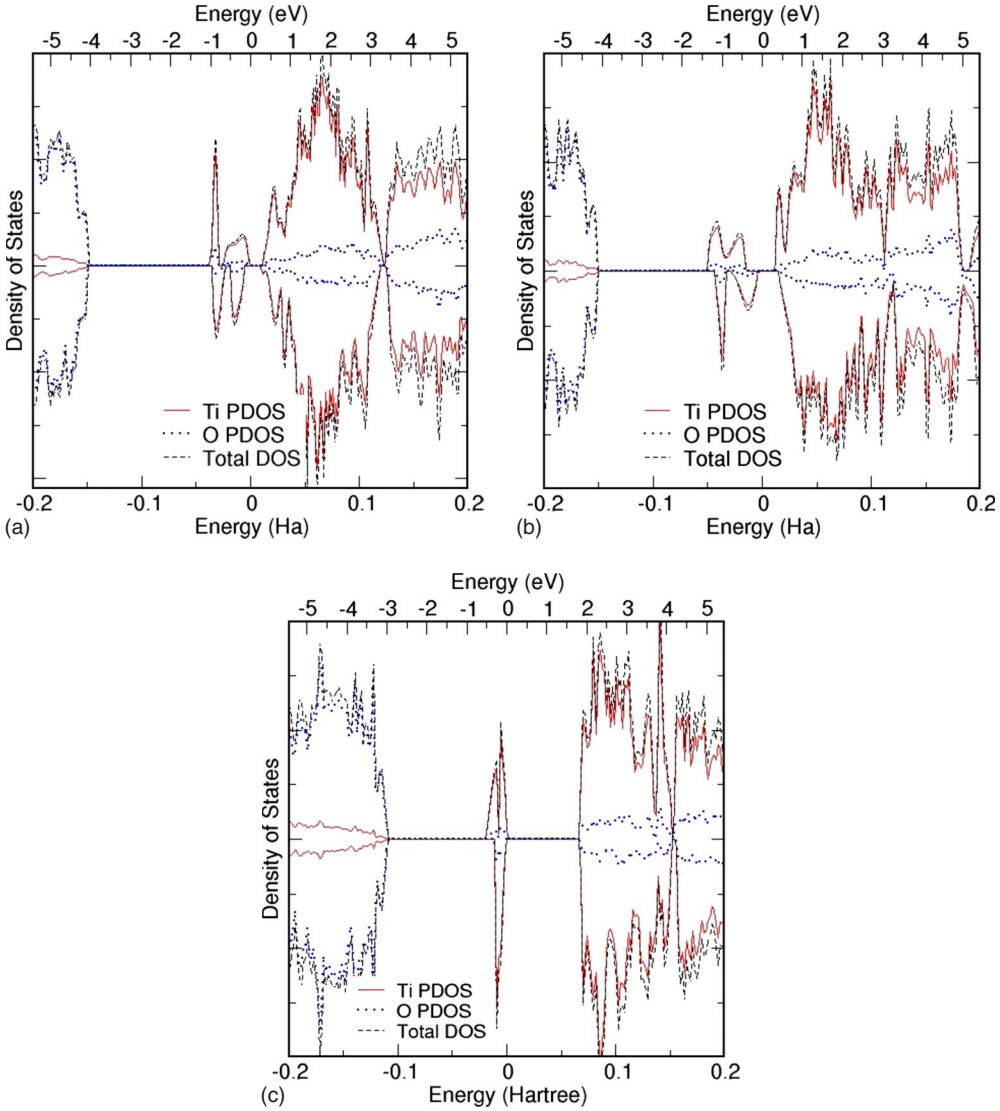


FIG. 4. (Color online) (a)–(c) are $Ti_4O_7$ electronic DOS and PDOS on the titanium and oxygen atoms. (a) shows the DOS at the high-temperature phase ($T>298$ K), (b) indicates the DOS at the intermediate phase ($T<140$ K), and (c) represents the DOS in the low-temperature phase ($T<120$ K).

obtained from optical transmission data. Kaplan's low-temperature band-gap value was obtained from the absorption threshold in a transmission vs wavelength curve, measured at 105 K. The measurements were performed in the energy range 0.3 to 0.2 eV.

According to our theoretical results for the DOS at 120 K—Fig. 4(c)—the fundamental band gap in the low-temperature phase is 1.5 eV. This is larger than the experimentally observed, but it might reflect the fundamental band gap of the material: the absorption observed by Kaplan might be due to alternative absorption processes within the energy range below 1 eV, such as the ones described below.

Lakkis *et al.*[8] proposed energy-level scheme for the $Ti^{3+}$ in the low-temperature phase. As a first approximation, they did not consider any possible broadening of the atomic or molecular levels into bands. They analyzed the crystalline field splitting due to a cubic field (perfect octahedral around the Ti): the fivefold *d* orbital is split into a triplet $t_{2g}$ and a doublet $e_g$. In turn, the orthorhombic component of the field (distorted octahedra) splits the $t_{2g}$ into three orbital singlets whose energy separation is around 0.4 eV. Energy absorption due to electrons being excited within states is suggested to be an atomic absorption mechanism.

Lakkis *et al.*[8] also suggested that a covalent bond existed between the $Ti^{3+}$ ions forming the dimers, and that the splitting of the bonding singlet and antibonding triplet was approximately 0.3 eV. This is an absorption mechanism that could explain the low-temperature optical absorption.

Another energy absorption mechanism was documented by Degiorgi *et al.*[30] They presented infrared optical measurements on the $Ti_4O_7$ low-temperature phase, which detected four IR-active phonon modes located around 34, 43, 62, and 78 meV.

Here we propose another possible absorption mechanism, which also involves spin flipping. For the low-temperature phase, we calculated the total energy of an hypothetical ferromagnetic state: the energy that would be necessary for changing from the antiferromagnetic to this hypothetical fer-

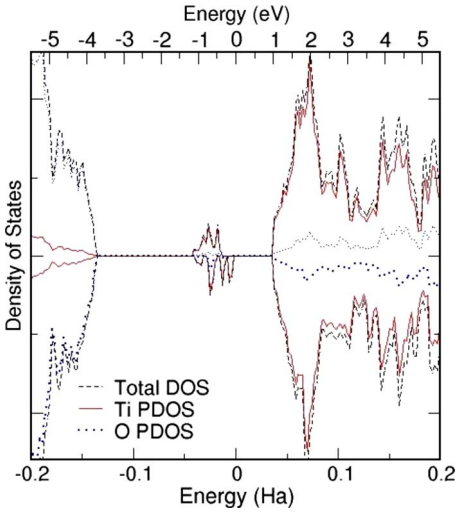


FIG. 5. (Color online) Electronic DOS and PDOS at the titanium and oxygen atoms for the Marezio and Page (Ref. 7) 140 K structure.

romagnetic state is 0.3 eV per $Ti_4O_7$ unit cell, which is the energy required to flip two spins.

Therefore, this disagreement within the experimental evidence could be suggesting that the value for the low-temperature band gap was underestimated: our theoretical value for the band gap might be reflecting the fundamental band gap of the material.

## IV. CONCLUSIONS

We have performed hybrid exchange (B3LYP) density functional calculations on the $Ti_4O_7$ Magnéli phase using the CRYSTAL code. Our results allowed for a consistent description of the high-temperature ($T \geq 298$ K) phase, the intermediate temperature (120 K $\leq T \leq 140$ K) phase and the low-temperature ($T \leq 120$ K) phase.

We found that the $Ti_4O_7$ low-temperature phase, ($T \leq 120$ K), has an antiferromagnetic charge-ordered semiconducting solution. This state can be viewed as a bipolaronic state, with well ordered $Ti^{3+}$-$Ti^{3+}$ pairs. According to our results for the Marezio and Page[7] 140 K structure, some of these $Ti^{3+}$-$Ti^{3+}$ pairs disappear when (120 K $\leq T \leq 140$ K), calling into question the previous interpretation[8] of the intermediate phase as a one of disordered bipolarons.

The spin localization pattern at Marezio and Page[7] 140 K structure had some similarities with the one observed in the 120 K structure proposed by Marezio *et al.*:[5] the system is antiferromagnetic and the spin is localized in half of the titaniums composing the supercell. But the electronic structure at 140 K is not a bipolaronic state: there is a mixture of polarons and bipolarons, and the system has long-range order.

Therefore, the transport properties in the intermediate phase are not due to bipolarons mobility.

The proposal that the spin remains strongly localized in the intermediate and low-temperature phases—and delocalizes at room temperature—provides an explanation of $Ti_4O_7$ magnetic properties.

As regards the question to whether is our theoretical value of 1.5 eV for the fundamental band-gap reasonable, we believe that, to answer this question, it would be necessary to extend the range of experimental optical measurements to higher energies. Because although the absorption threshold in Kaplan's experiments[11] is at around 0.25 eV, this absorption might not be related with interband transitions.

## ACKNOWLEDGMENTS

The calculations performed for this work were carried out in the facilities of Imperial College High Performance Computing Service.[31] This work was funded by the EPSRC under the multiscale modeling approach to engineering functional coatings' initiative (EP/C524322/1).

*l.liborio@imperial.ac.uk

[1] L. A. Bursill and B. G. Hyde, Prog. Solid State Chem. **7**, 177 (1972).
[2] P. Waldner and G. Eriksson, CALPHAD: Comput. Coupling Phase Diagrams Thermochem. **23**, 189 (1999).
[3] R. F. Bartholomew and D. R. Frankl, Phys. Rev. **187**, 828 (1969).
[4] A. D. Inglis, Y. L. Page, P. Strobel, and C. M. Hurd, J. Phys. C **16**, 317 (1983).
[5] M. Marezio, D. B. McWhan, P. D. Dernier, and J. P. Remeika, J. Solid State Chem. **6**, 213 (1973).
[6] R. D. Shannon and C. T. Prewitt, Acta Crystallogr., B: Struct. Crystallogr. Cryst. Chem. **25**, 925 (1969).
[7] Y. Le Page and M. Marezio, J. Solid State Chem. **53**, 13 (1984).
[8] S. Lakkis, C. Schlenker, B. K. Chakraverty, and R. Buder, Phys. Rev. B **14**, 1429 (1976).
[9] J. S. Anderson and A. S. Khan, J. Less-Common Met. **22**, 219 (1970).
[10] N. Mott and A. S. Alexandrov, *Polarons & Bipolarons* (World Scientific, Singapore, 1995).
[11] D. Kaplan, C. Schlenker, and J. J. Since, Philos. Mag. **36**, 1275 (1977).
[12] M. Watanabe, W. Ueno, and T. Hayashi, J. Lumin. **122-123**, 393 (2007).
[13] L. Liborio and N. Harrison, Phys. Rev. B **77**, 104104 (2008).
[14] I. Leonov, A. N. Yaresko, V. N. Antonov, U. Schwingenschlögl, V. Eyert, and V. I. Anisimov, J. Phys.: Condens. Matter **18**, 10955 (2006).
[15] V. Eyert, U. Schwingenschlögl, and U. Eckern, Chem. Phys. Lett. **390**, 151 (2004).
[16] R. Dovesi *et al.*, *CRYSTAL06 User's Manual* (Università di Torino, Torino, 2006), www.crystal.unito.it
[17] J. Muscat, Ph.D. thesis, University of Manchester, 1999.
[18] J. Muscat, N. M. Harrison, and G. Thornton, Phys. Rev. B **59**, 2320 (1999).
[19] J. Muscat, V. Swamy, and N. M. Harrison, Phys. Rev. B **65**,

224112 (2002).
[20] G. Mallia and N. M. Harrison, Phys. Rev. B **75**, 165201 (2007).
[21] A. D. Becke, J. Chem. Phys. **98**, 5648 (1993).
[22] C. Pisani, R. Dovesi, and C. Roetti, *Hartree-Fock ab initio Treatment of Crystalline Systems*, Lecture Notes in Chemistry Vol. 48 (Springer-Verlag, Heidelberg, 1988).
[23] Results for the 140 K structure are included for completeness: the crystalline structure for the $Ti_4O_7$ intermediate phase is given by the results of Marezio and Page (Ref. 7).
[24] J. K. Burdett, T. Hughbanks, G. J. Miller, J. W. Richardson, and J. V. Smith, J. Am. Chem. Soc. **109**, 3639 (1987).
[25] L. N. Mulay and W. J. Danley, J. Appl. Phys. **41**, 877 (1970).
[26] S. Blundell, *Magnetism in Condensed Matter* (Oxford University Press, New York, 2004).
[27] L. K. Keys and L. N. Mulay, Phys. Rev. **154**, 453 (1967).
[28] The so-called Pauli susceptibility is typical of metals (Ref. 26).
[29] M. Abbate, R. Potze, G. A. Sawatzky, C. Schlenker, H. J. Lin, L. H. Tjeng, C. T. Chen, D. Teehan, and T. S. Turner, Phys. Rev. B **51**, 10150 (1995).
[30] L. Degiorgi, P. Watcher, and C. Schlenker, Physica B **164**, 305 (1990).
[31] http://www.imperial.ac.uk/ict/services/teachingandresearchservices/highperformancecomputing